KERNFORSCHUNGSZENTRUM KARLSRUHE

Juli 1969 KFK 1084

Zyklotron-Laboratorium

Orbit Dynamics of Isochronous Cyclotrons with Separate Homogeneous Field Magnets

G. Schatz

GESELLSCHAFT FÜR KERNFORSCHUNG M.B.H.

KARLSRUHE

NUCLEAR INSTRUMENTS AND METHODS 72 (1969) 29–34; © NORTH-HOLLAND PUBLISHING CO.

ORBIT DYNAMICS OF ISOCHRONOUS CYCLOTRONS WITH SEPARATE HOMOGENEOUS FIELD MAGNETS

G. SCHATZ

Zyklotron-Laboratorium, Kernforschungszentrum Karlsruhe

Received 6 February 1969

Explicit expressions are derived for the orbit properties of isochronous cyclotrons with separate homogeneous field magnets by use of the matrix method and the hard edge approximation. The results hold for arbitrary shapes of the magnet boundaries (subject to the condition of isochronism). As a design example a 50 to 310 MeV proton accelerator is considered in more detail.

1. Introduction

Recently, isochronous cyclotrons with separated magnets have received increased interest. Besides the machines of this type which are either under construction[1]) or definitely proposed[2]) isochronous ring accelerators have been studied as an alternative to the Separated Orbit Cyclotron[3]) and for accelerating heavy ions[4,5]).

For light projectiles, the main advantage of a separated magnet structure lies in the field of beam extraction from the accelerator: A high energy gain per turn can be achieved by inserting separate rf structures into the field free sections between the magnets, and, in addition, the radial width of a single orbit can be reduced by exciting one or several of the rf cavities at the third harmonic frequency ("flat-topping the rf"). The latter aspect has been studied in detail by Gordon[3]) to whom we therefore refer for details. For heavy ions a separated magnet cyclotron offers the possibility of increasing the ionic charge by stripping at an intermediate energy before injection into the ring[5]).

In a recent paper, Gordon[6]) has studied the orbit properties of a separated magnet structure with radial sectors where isochronism is maintained by a radial increase of field strength in the magnets. This paper presents the results of a similar study of the case of homogeneous field magnets where isochronism is achieved by increasing the azimuthal width of the magnets with increasing radius. Explicit expressions can be derived for the number of betatron oscillations per turn for this case. Some of the results of this paper have been quoted without proof in a preceding publication[5]).

2. Basic assumptions

It is assumed that the guiding field is produced by N identical homogeneous field magnets with N field-free sections in between. The hard edge approximation is assumed to be valid such that the orbit is composed of circular and straight sections. The number of betatron oscillations per revolution can then be determined by use of the matrix method [cf., e.g., Livingood[7])]. The transfer matrix of one period of the magnetic field is the product of the matrices corresponding to the magnetic sector ($\mathbf{M}_m$) and to the fieldfree sector ($\mathbf{M}_f$), respectively. The matrix $\mathbf{M}_f$ only depends on the length l of the straight section of the orbit between two magnets and is given by

$$\mathbf{M}_f = \begin{pmatrix} l & 1 \\ 0 & 1 \end{pmatrix}. \qquad (1)$$

The magnet can be replaced by a sector magnet with straight edges which coincide with the tangents to the magnet boundaries at the entrance and exit of the orbit (cf. fig. 1). The transfer matrix corresponding to such a sector magnet is given by Steffen[8]), e.g. Using the notation of fig. 1 we obtain the following expressions for the radial and axial movements, respectively:

$$\mathbf{M}_{mr} = \begin{bmatrix} \cos[(2\pi/N)-\gamma_1](\cos\gamma_1)^{-1} & r\sin(2\pi/N) \\ -(1+\mathrm{tg}\gamma_1\,\mathrm{tg}\gamma_2)\sin[(2\pi/N)-\gamma_1+\gamma_2]\,\{r\cos(\gamma_1-\gamma_2)\}^{-1} & \cos[(2\pi/N)+\gamma_2](\cos\gamma_2)^{-1} \end{bmatrix}, \qquad (2a)$$

$$\mathbf{M}_{mz} = \begin{bmatrix} 1-(2\pi/N)\mathrm{tg}\gamma_1 & 2\pi r/N \\ r^{-1}[\mathrm{tg}\gamma_2-\mathrm{tg}\gamma_1-(2\pi/N)\mathrm{tg}\gamma_1\,\mathrm{tg}\gamma_2] & 1+(2\pi/N)\mathrm{tg}\gamma_2 \end{bmatrix}. \qquad (2b)$$

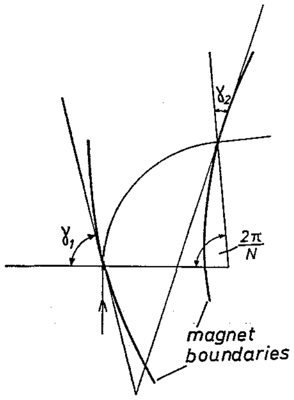

Fig. 1. Orbit section in one magnet sector. The angles γ_1 and γ_2 are defined positive for the situation shown in this figure.

In these expressions, the signs of γ_1 and γ_2 are chosen in such a way that both angles are positive for the situation shown in fig. 1. Furthermore we have taken into account that the total angle of deflection of the orbit in one magnet equals $2\pi/N$. From these expressions the numbers of radial and axial betatron oscillations per turn, ν_r and ν_z, respectively, can be calculated[7]):

$$\cos(\nu_{r,z}\cdot 2\pi/N) = \tfrac{1}{2}\mathrm{Tr}(\mathbf{M}_\mathrm{f}\cdot \mathbf{M}_{\mathrm{m}r,z}). \qquad (3)$$

These equations reduce the problem of beam stability to the problem of determining the geometrical quantities γ_1, γ_2 and l.

3. The non-relativistic case

For all of this section, the relativistic mass increase is neglected. The results may be of interest for a cyclotron accelerating heavy ions to energies below 10 MeV/nucleon as the mass increase then amounts to less than 1%. The azimuthal magnet boundaries are assumed to

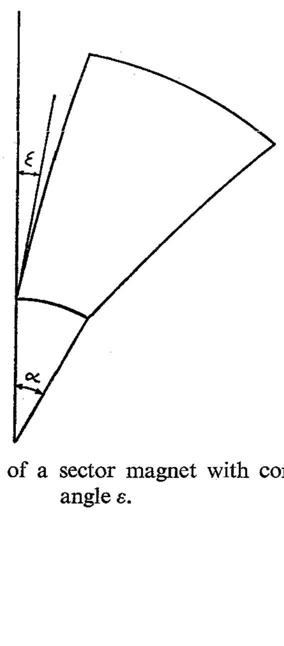

Fig. 2. Cross section of a sector magnet with constant spiral angle ε.

be given by logarithmic spirals the equation of which is

$$\rho = \rho_0 \exp(\phi \cdot \mathrm{ctg}\,\varepsilon), \qquad (4)$$

in polar coordinates ρ,ϕ. For these spirals, the angle ε between the magnet boundary and a straight line through machine center is independent of radius. Let α be the angle occupied by one magnet*. The field-free sections then occupy the angle $(2\pi/N)-\alpha$. Fig. 2 shows a cross section of one magnet.

3.1. Calculation of the equilibrium orbit

Let r be the radius of curvature of the orbit in the magnetic field and s the distance between machine center and the point of entrance of the orbit into the magnet sector. As the equilibrium orbit is strictly periodic a relation connecting r,s and the angles α and ε has to exist. Fig. 3 shows the section of the orbit in one period of the magnetic field. The points A, B, and C are

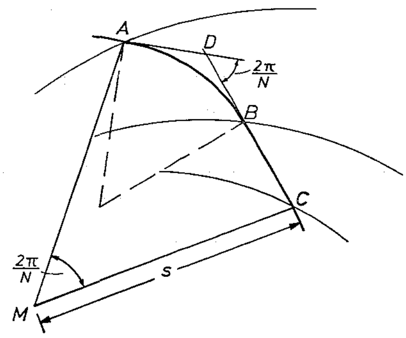

Fig. 3. Orbit section in one period of the magnetic field.

successive points of intersection of the orbit with the magnet boundaries, point D is the point of intersection of the straight lines which coincide with the straight orbit sections. Due to the periodicity of orbit and magnetic field we obtain $\overline{AM} = \overline{CM} = s$. It is less obvious that point B has the same distance from M as A and C. This can be shown by the following geometrical consideration:

As the orbit is deflected by the angle $2\pi/N$ in one magnet sector the sum of the angles $\angle$ADC and $\angle$CMA equals π. Consequently, the four points A, C, D and M are situated on one circle. For the sake of clarity, the relevant parts of fig. 3 are repeated in fig. 4. As the two intervals $\overline{AM}$ and $\overline{CM}$ have equal size the same holds for the two angles $\angle$ADM and $\angle$CDM. Also, the two intervals $\overline{AD}$ and $\overline{BD}$ have equal length for reasons of symmetry as is evident from fig. 3. Then

* The angle α is connected to the magnet fraction f in Gordon's paper by $\alpha = 2\pi f/N$.

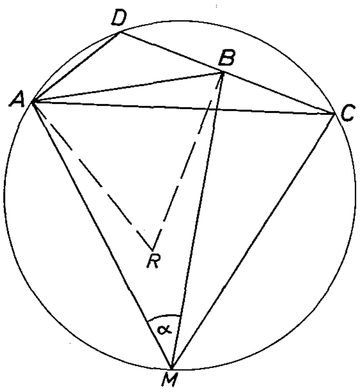

Fig. 4. Part of fig. 3 with all quantities relevant to the calculation of the equilibrium orbit.

the two triangles ADM and BDM are congruent which establishes the said proposition $\overline{BM} = s$.

As the angle $\angle$ AMB equals α we can read from fig. 3 the relation

$$s\sin(\tfrac{1}{2}\alpha) = r\sin(\pi/N), \qquad (5)$$

which characterizes the equilibrium orbit and is evidently independent of ε.

3.2. Orbit stability

According to the results of section 2 we now have to determine the quantities l, γ_1 and γ_2. From fig. 4 we see immediately

$$l = 2s\sin[(\pi/N)-\tfrac{1}{2}\alpha] =$$
$$= 2r\sin(\pi/N)\sin[(\pi/N)-\tfrac{1}{2}\alpha](\sin\tfrac{1}{2}\alpha)^{-1}. \qquad (6)$$

The point R in fig. 4 represents the centre of the circular part of the orbit between A and B. As the angle between the magnet boundary and the straight line $\overline{AM}$ equals ε we obtain the following expressions of the angles:

$$\gamma_1 = \tfrac{1}{2}(\pi-\alpha)-\tfrac{1}{2}[\pi-(2\pi/N)]+\varepsilon = (\pi/N)-\tfrac{1}{2}\alpha+\varepsilon, \qquad (7a)$$

$$\gamma_2 = -(\pi/N)+\tfrac{1}{2}\alpha+\varepsilon. \qquad (7b)$$

By evaluating eq. (3) we get

$$\cos(\nu_r\cdot 2\pi/N) = \cos(2\pi/N)-\{1-\cos(2\pi/N)\}\cdot$$
$$\cdot\{1-\cos[(2\pi/N)-\alpha]\}\cdot$$
$$\cdot\{\cos(2\varepsilon)+\cos[(2\pi/N)-\alpha]\}^{-1}, \qquad (8a)$$

$$\cos(\nu_z\cdot 2\pi/N) = 1-\{(\pi/N)+\sin(\pi/N)\sin[(\pi/N)-\tfrac{1}{2}\alpha]\cdot$$
$$\cdot(\sin\tfrac{1}{2}\alpha)^{-1}\}\{\mathrm{tg}[(\pi/N)-\tfrac{1}{2}\alpha+\varepsilon]+$$
$$+\mathrm{tg}[(\pi/N)-\tfrac{1}{2}\alpha-\varepsilon]\}+$$
$$+(2\pi/N)\sin(\pi/N)\sin[(\pi/N)-\tfrac{1}{2}\alpha]\cdot$$
$$\cdot(\sin\tfrac{1}{2}\alpha)^{-1}\mathrm{tg}[(\pi/N)-\tfrac{1}{2}\alpha+\varepsilon]\cdot$$
$$\cdot\mathrm{tg}[(\pi/N)-\tfrac{1}{2}\alpha-\varepsilon]. \qquad (8b)$$

For $\varepsilon = 0$ these equations are identical to eqs. (38) in a recent publication by Gordon[6]). As an example, fig. 5 shows the number of radial and axial betatron oscillations per turn for $N = 6$ and two different spiral angles.

4. The general case

In this section we drop two simplifying assumptions made in the preceding one:

a. We take the relativistic mass increase into account;
b. We allow arbitrary shapes of the entrance boundaries of the magnets.

We still make use of the hard edge approximation and of the matrix method.

Let $\phi = \beta(s)$ be the equation of the entrance boundary of a magnet in polar coördinates ϕ, s and let α and s have the same meaning as in section 3. The angle β is considered an arbitrary function of s which is specified later on to obtain optimum orbit properties. The angle α now becomes a function of s, too, if isochronism is to be maintained.

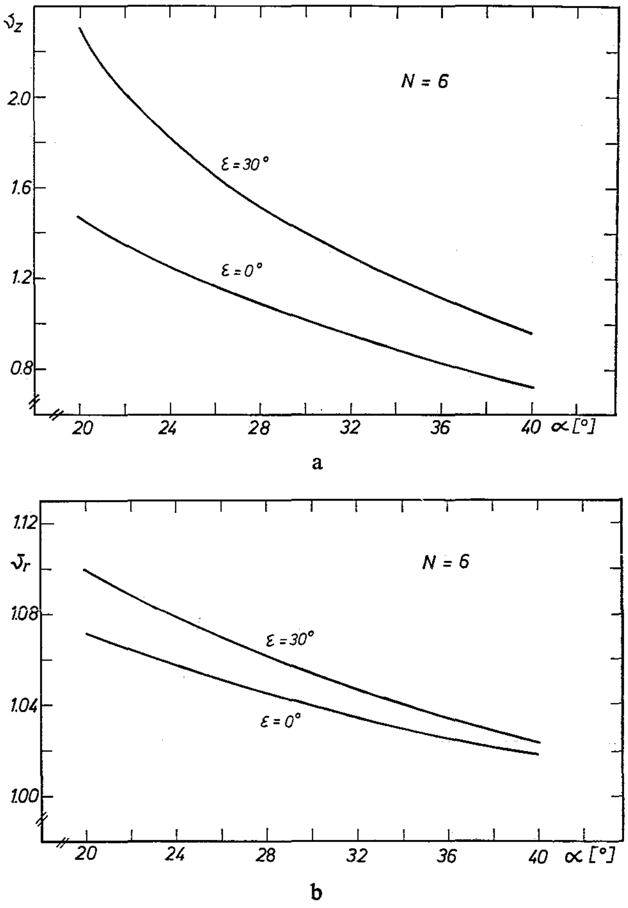

Fig. 5. Dependence of (a) ν_z and (b) ν_r on the angles α and ε for a nonrelativistic cyclotron with 6 magnets.

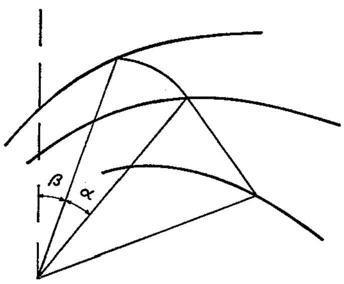

Fig. 6. Orbit section in one period of the magnetic field with definition of the angles α and β.

Fig. 6 shows a part of the orbit in one period of the magnetic field. In section 3 it has been proved that the equilibrium orbit intersects all magnet boundaries at the same distance from machine centre. The proof was based on the following two presuppositions:
a. The equilibrium orbit is periodic with $2\pi/N$;
b. It is deflected by the angle $2\pi/N$ in one magnet.

The result therefore holds in the general case. As a consequence eqs. (5) and (6) also hold under the assumptions of this section. Expressing the radius r by the particle energy we rewrite eq. (5)

$$s\sin(\tfrac{1}{2}\alpha) = (c/\omega)(\gamma^2-1)^{\frac{1}{2}}\sin(\pi/N). \qquad (9)$$

Here, c is the velocity of light, ω the low energy angular frequency of the particles moving in the homogeneous field of the magnets and γ is the ratio of total and rest energies of the particle.

4.1. The condition of isochronism

Isochronism determines the dependence of α on s. Let $L(\gamma)$ be the length of the equilibrium orbit of energy γ and τ the time of revolution of the particles. Isochronism then requires that

$$\tau = L/v = \text{const.}$$

where v is the particle velocity. The length of the equilibrium orbit is given by

$$L = N[(2\pi r/N)+l] = 2\pi r + 2Ns\sin[(\pi/N)-\tfrac{1}{2}\alpha]. \qquad (10)$$

Here, l is the length of the straight orbit section between two magnets. By use of eq. (5) this yields

$$\tau = (2\pi r/v)\{1+(N/\pi)\sin(\pi/N)\sin[(\pi/N)-\tfrac{1}{2}\alpha]\cdot \cdot(\sin\tfrac{1}{2}\alpha)^{-1}\}. \qquad (11)$$

The quantity r/v equals γ/ω. Equating $\tau(\gamma=1)$ with $\tau(\gamma)$ from eq. (11) we obtain a relation between γ and α:

$$\gamma\{1+(N/\pi)[\sin(\pi/N)]^2\operatorname{ctg}(\tfrac{1}{2}\alpha) - (N/\pi)\sin(\pi/N)\cos(\pi/N)\} = 1+(N/\pi)[\sin(\pi/N)]^2\operatorname{ctg}(\tfrac{1}{2}\alpha_0) - (N/\pi)\sin(\pi/N)\cos(\pi/N), \qquad (12)$$

where $\alpha_0 = \alpha(s=0)$. For numerical calculations it is more convenient to use instead of eq. (12) the following equivalent expression

$$\gamma(\gamma-1)^{-1}\{\operatorname{ctg}(\tfrac{1}{2}\alpha_0)-\operatorname{ctg}(\tfrac{1}{2}\alpha)\} = (\pi/N)[\sin(\pi/N)]^{-2}+\operatorname{ctg}(\tfrac{1}{2}\alpha_0)-\operatorname{ctg}(\pi/N). \qquad (13)$$

The right hand side of this equation is evidently independent of γ and α. Eqs. (9) and (13) determine the width of the magnet once the parameters N and α_0 have been chosen.

4.2. Orbit stability

The entrance and exit boundaries of the magnets are given by the eqs. $\phi=\beta(s)$ and $\phi=\beta(s)+\alpha(s)$, respectively, in polar coordinates. Hence we obtain for the spiral angles ε_1 and ε_2 of the boundaries

$$\operatorname{tg}\varepsilon_1 = s(\mathrm{d}\beta/\mathrm{d}s), \qquad (14a)$$

$$\operatorname{tg}\varepsilon_2 = s[(\mathrm{d}\beta/\mathrm{d}s)+(\mathrm{d}\alpha/\mathrm{d}s)] = \operatorname{tg}\varepsilon_1 + s(\mathrm{d}\alpha/\mathrm{d}s). \qquad (14b)$$

While $\beta(s)$ is a function which can still be chosen in order to optimize a special design $\mathrm{d}\alpha/\mathrm{d}s$ must be calculated from the expressions given above. It is advantageous to consider γ as the independent variable and to write

$$\mathrm{d}\alpha/\mathrm{d}s = (\mathrm{d}\alpha/\mathrm{d}\gamma)(\mathrm{d}s/\mathrm{d}\gamma)^{-1}.$$

This expression can be determined by differentiating eqs. (9) and (13) with respect to γ. A tedious but straightforward calculation then results in

$$\operatorname{tg}\varepsilon_2 = \operatorname{tg}\varepsilon_1 + 2\{\gamma^2(\gamma+1)^{-1}\cdot \cdot\sin\tfrac{1}{2}\alpha_0[\sin\tfrac{1}{2}\alpha\sin\tfrac{1}{2}(\alpha-\alpha_0)]^{-1}-\operatorname{ctg}\tfrac{1}{2}\alpha_0\}^{-1}. \qquad (15)$$

By analogy with eq. (7) we obtain for the angles γ_1 and γ_2

$$\gamma_1 = (\pi/N)-\tfrac{1}{2}\alpha+\varepsilon_1, \qquad (16a)$$

$$\gamma_2 = -(\pi/N)+\tfrac{1}{2}\alpha+\varepsilon_2. \qquad (16b)$$

A similar calculation as in section 3 then leads to

$$\cos(\nu_r\cdot 2\pi/N) = \{\cos(\alpha+\varepsilon_2-\varepsilon_1) + \cos(2\pi/N)\cos(\varepsilon_1+\varepsilon_2) - 2\sin(\pi/N)\sin[(\pi/N)-\tfrac{1}{2}\alpha]\cdot \cdot\sin(\alpha+\varepsilon_2-\varepsilon_1)(\sin\tfrac{1}{2}\alpha)^{-1}\}\cdot \cdot\{\cos(\varepsilon_1+\varepsilon_2) + \cos[(2\pi/N)-\alpha+\varepsilon_1-\varepsilon_2]\}^{-1}, \qquad (17a)$$

$$\cos(\nu_z \cdot 2\pi/N) = 1 - \{\mathrm{tg}[(\pi/N) - \tfrac{1}{2}\alpha + \varepsilon_1] + \mathrm{tg}[(\pi/N) - \tfrac{1}{2}\alpha - \varepsilon_2]\}\{(\pi/N) + \sin(\pi/N)\sin[(\pi/N) - \tfrac{1}{2}\alpha]\cdot (\sin\tfrac{1}{2}\alpha)^{-1}\} + (2\pi/N)\sin(\pi/N)\cdot \sin[(\pi/N) - \tfrac{1}{2}\alpha](\sin\tfrac{1}{2}\alpha)^{-1}\cdot \mathrm{tg}[(\pi/N) - \tfrac{1}{2}\alpha + \varepsilon_1]\mathrm{tg}[(\pi/N) - \tfrac{1}{2}\alpha - \varepsilon_2]. \quad (17b)$$

It can easily be shown that eqs. (17) reduce to eqs. (8) if $\varepsilon_1 = \varepsilon_2 = \varepsilon$.

The sequence of eqs. (13), (14), (15) and (17) can now be used to determine all orbit properties at different energies once the parameters N and α_0 and the function $\beta(s)$ have been chosen. The shape of the magnets is determined by $\beta(s)$ and eqs. (9) and (13).

4.3. Determination of the magnet shape from ν_z

It should be pointed out that the equations given above can be used to determine the spiral angle ε_1 and hence the magnet shape from a prescribed value of ν_z. It is therefore possible – in principle at least – to choose an arbitrary dependence of ν_z on the particle energy and to calculate the corresponding magnet shape. Of course, the corresponding values of ν_r or practical considerations may severely restrict the choice of ν_z values.

The relevant equations are obtained by eliminating ε_2 from eqs. (15) and (17b). This results in a second order equation for $\mathrm{tg}\,\varepsilon_1$:

$$2\{[\pi(t-b)/N] + tb - [t\sin(\nu_z\pi/N)]^2\}(\mathrm{tg}\,\varepsilon_1 + a)\mathrm{tg}\,\varepsilon_1 + (2t - a + at^2)[b + (\pi/N)] + t(t-a)(2\pi b/N) + -2(1+at)[\sin(\nu_z\pi/N)]^2 = 0, \quad (18)$$

where the following abbreviations have been used

$$t = \mathrm{tg}[(\pi/N) - \tfrac{1}{2}\alpha],$$
$$a = \mathrm{tg}\,\varepsilon_2 - \mathrm{tg}\,\varepsilon_1 \text{[cf. eq. (15)]},$$
$$b = \sin(\pi/N)\sin[(\pi/N) - \tfrac{1}{2}\alpha](\sin\tfrac{1}{2}\alpha)^{-1}.$$

The quantities a, b and t only depend on α and the parameters α_0 and N. Once the parameters α_0 and N have been chosen α as well as s are determined by the particle energy γ via eqs. (9) and (13). Eq. (18) then determines ε_1, and the magnet shape, i.e. the angle β, is obtained by integrating eq. (14a) with respect to s.

5. Design example

A very simple example is obtained by chosing the entrance edge of each magnet as a straight line through machine centre, i.e. by putting $\beta = \varepsilon_1 = 0$. This design

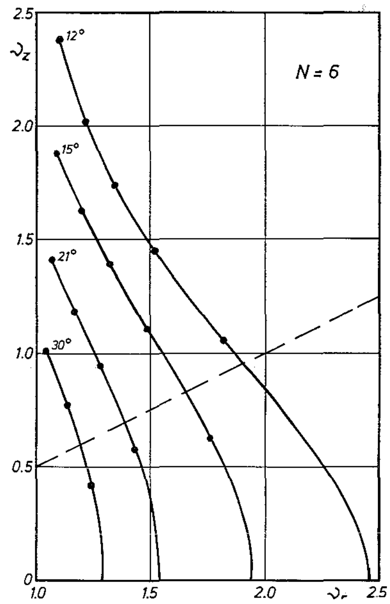

Fig. 7. Orbit frequencies ν_r and ν_z for a cyclotron with $N = 6$ and straight radial entrance edges of the magnets. The curves start on top at zero energy ($\gamma = 1$), the dots represent intervals of $\Delta\gamma = 0.1$, and the parameters give the value of the angle α_0. The dashed line indicates the resonance $2\nu_z = \nu_r$.

has of course considerable advantages from the point of view of manufacture. Fig. 7 shows a plot of ν_z against ν_r for $N = 6$ and several values of α_0. The curves start on top at $\gamma = 1$. With increasing γ, ν_r increases while ν_z decreases. The dots along the lines represent intervals of $\Delta\gamma = 0.1$. The dashed line indicates the coupling resonance $2\nu_z = \nu_r$.

The question of resonances has been discussed extensively by Gordon[6]). As the dependence of ν_r and ν_z is very similar to his results we confine ourselves to

Table 1

Orbit properties and dimensions of an isochronous ring accelerator with straight radial entrance edges of the magnets. The main parameters have the values of N=6 and α_0=15°, and the dimensions refer to a proton accelerator with a field of 15.7 kG in the magnets.

γ	α (deg)	s (m)	ν_r	ν_z
1.00	15.00	0	1.092	1.877
1.05	15.78	2.33	1.145	1.749
1.10	16.56	3.18	1.200	1.628
1.15	17.34	3.77	1.258	1.510
1.20	18.13	4.21	1.322	1.388
1.25	18.91	4.56	1.396	1.258
1.30	19.70	4.86	1.487	1.107
1.35	20.49	5.10	1.603	0.917
1.40	21.28	5.31	1.766	0.629

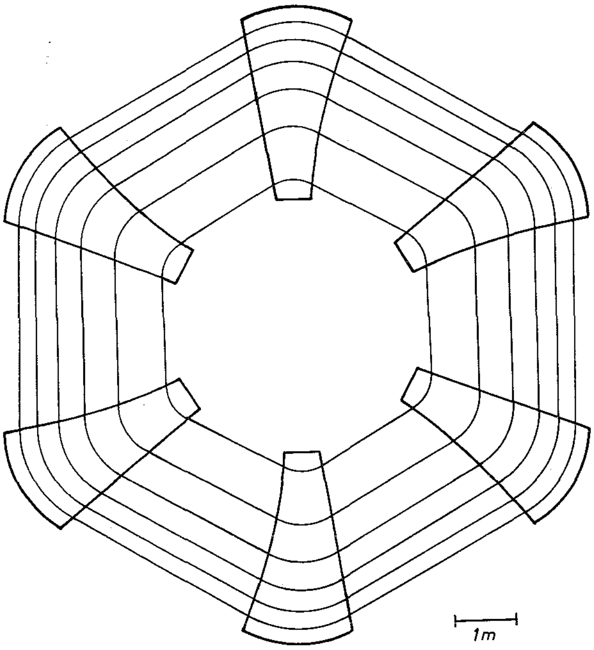

Fig. 8. Lay-out of a 50 to 300 MeV proton accelerator with straight radial entrance edges of the magnets and $\alpha_0 = 15°$. Equilibrium orbits are drawn at 50 MeV intervals. The orbit properties of this accelerator are given in table 1.

some short remarks and refer to his work for a more detailed discussion. The most serious resonance to be taken into account is the resonance $\nu_z = 1$. As this resonance cannot be crossed during acceleration one is restricted to operate in the regions $1 < \nu_z < 2$ or $\nu_z < 1$. As fig. 7 shows both regions can be used depending on the choice of α_0 and on the energy range of the accelerator.

As a specific example the case of $N = 6$ and $\alpha_0 = 15°$ are considered in more detail. The results of the calculation are summarized in table 1 where the dimensions refer to a proton accelerator with a magnetic field strength of 15.7 kG in the magnets. As can be seen this choice of parameters seems to be suitable for a proton accelerator from 50 to about 350 MeV. Fig. 8 shows the lay-out of a 50 to 300 MeV proton accelerator.

6. Conclusion

It was shown that for the case of homogeneous field magnets the orbit properties of a separated magnet isochronous cyclotron can be determined without solving differential equations of motion. The important approximation made to obtain explicit expression for the orbit properties is the hard edge approximation. As the width of the stray field region of the magnets constitutes a larger portion of the orbit at low energies the approximation is expected to be more precise at higher energies. Experience shows[6]) that ν_z values are lower in reality than estimated by this approximation. Nevertheless, it is felt that the expressions derived here are sufficiently precise for serving as a guide line in choosing the parameters of a special design which then should be considered more closely by more exact methods. The results obtained are qualitatively very similar to recently published results for similar accelerators[6]).

I thank Prof. M. M. Gordon, Michigan State University, for making his results available to me prior to publication. I am indebted to Mrs. G. Hoffmann for preparing the drawings and for carrying out the numerical calculations.

References

[1]) J. P. Blaser and H. A. Willax, IEEE Trans. Nucl. Sci. **NS-13** no. 4 (1966) 194.
[2]) 200 MeV multiparticle multiple-stage cyclotron, a proposal to the US NSF, Department of Physics, Indiana University, (1968); A. A. Glasov et. al. JINR-R 3932.
[3]) M. M. Gordon, Nucl. Instr. and Meth. **58** (1968) 245.
[4]) V. P. Dzelepov, V. P. Dmitrievskij, B. I. Zamolodcikov and V. V. Kol'ga, Proc. 6th Intern. Conf. *High Energy Accelerators* (Cambridge, 1967) CEAL-2000, p. 295; Atomn. Energ. **24** (1968) 323.
[5]) G. Schatz, Nucl. Instr. and Meth. **67** (1969) 103.
[6]) M. M. Gordon, Ann. Phys. (N.Y.) **50** (1968) 571.
[7]) J. J. Livingood, *Cyclic Particle Accelerators* (Princeton, 1961) p. 42.
[8]) K. G. Steffen, *High Energy Beam Optics* (New York, 1965) p. 100.